Article:
Ali, M, Mahmud, T, Heggs, P et al. (6 more authors) (2017) Residence Time Distribution of Glass Ballotini in Isothermal Swirling Flows in a Counter-Current Spray Drying Tower. Powder Technology, 305. pp. 809-815. ISSN 0032-5910

https://doi.org/10.1016/j.powtec.2016.10.023

Accepted for publication in Powder Technology on 13 October 2016
doi:10.1016/j.powtec.2016.10.023

Residence Time Distribution of Glass Ballotini in Isothermal Swirling Flows in a Counter-Current Spray Drying Tower

Muzammil ALI [1], Tariq MAHMUD[1*], Peter HEGGS[1], Mojtaba GHADIRI[1], Andrew BAYLY[1], Mark CROSBY[2], Hossein AHMADIAN[2], Luis MARTINDEJUAN[2] and Zayeed ALAM[2]

[1]School of Chemical and Process Engineering, University of Leeds, Leeds LS2 9JT, UK

[2]P&G Technical Centres Ltd., Longbenton, Newcastle Upon Tyne NE12 9BZ, UK

*Corresponding author: Tel.: +44 (0)113 3432431; Email: T.Mahmud@leeds.ac.uk

Keywords: Residence time distribution, CFD, Spray Drying, Multiphase Flow Modelling

Abstract: The particle residence time in counter-current spray drying towers has a significant influence on the moisture content of the powder exiting the tower. Therefore, the reliability of predictions of residence time by numerical methods is highly desirable. A combined experimental and computational fluid dynamics investigation is reported for the prediction of the residence time distributions of glass beads with a narrow size range of 300-425 μm in a counter-current tower with isothermal swirling flows of air. The particle-wall collision is taken into account using a rough-wall collision model. Overall, a reasonably good agreement is obtained between the measurements and predictions. Consideration of wall roughness results in greater axial dispersion of particles in the tower compared to a smooth wall assumption. The rough particle-wall collision is important for a reliable prediction of residence time distributions. In addition, analysis of the results infers that the clustering effect of particles on drag and particle-particle interactions are important and should be investigated in a future study.

1. Introduction

Counter-current spray drying towers are used for the production of thermally stable particulate products such as detergent and ceramic powders. It involves drying of atomised solution or slurry into dry particles by a hot gas, typically combustion product of a fuel gas burnt with atmospheric air. The solution or slurry is sprayed into the drying tower using an atomizer. The atomized droplets come in contact with a turbulent, swirling hot gas flowing in the opposite direction and heat, mass and momentum exchange occurs between the phases. Moisture evaporates from the droplets resulting in the formation of solid particles.

It is highly desirable to optimise the design parameters, such as the tower diameter and height, type of spray nozzle, and hot air injection nozzle angle and position, and operating conditions, such as the feed temperature, moisture, inject pressure, mass flow and droplet size, for the production of particles with required properties as well as stable and energy efficient operations. The optimisation is generally carried out using experimental trials which are expensive and time consuming. The use of computational models for optimization has been limited due to the complexity of spray drying process as it involves billions of poly-dispersed droplets/particles interacting with complex gas flow patterns that affect their trajectories and residence times. Additionally, there are interactions between the droplets and particles resulting in coalescence, agglomeration and breakage as well as interactions with the tower wall resulting in deposition, re-entrainment of deposited material, and breakage of particles. If the deposited material is exposed to a high temperature for a prolonged period of time, it may result in combustion, hence posing safety issues. Therefore, the spray drying tower needs to be inspected for material build-up on the wall and cleaned periodically, which requires shutting down the plant resulting in the loss of production (Masters, 1985).

Computational fluid dynamics (CFD) is considered as an appropriate technique for the modelling of such complex processes in spray drying towers. The extent of drying of droplets/particles of various sizes and hence the final powder characteristics including size, temperature and moisture content depend on their

residence time distributions (RTD). Longer residence times can lead to charring and thermal degradation; on the contrary, if the particles do not spend sufficient time in the tower then they may come out with excessive moisture causing sticking and cake formation. It is therefore crucial that a CFD predictive methodology must provide an accurate estimation of RTD for the complete size distribution in the spray drying tower. A number of studies have been published in the last three decades utilizing CFD for the modelling of counter-current spray drying towers (e.g., Crowe, 1983; Livesley *et al.*, 1992; Zbicinski and Zietara, 2004; Wawrzyniak *et al.*, 2012; Wawrzyniak *et al.*, 2014; Jaskulski *et al.*, 2014; Ali *et al.*, 2015). However, to the best of authors' knowledge, there is no direct comparison of the predicted RTD with measurements in such towers reported in the literature, including the above references. In contrast, several studies have been published on the measurement and prediction of RTDs in co-current spray dryers. In one of the first reported studies, Pham and Keey (1997) carried out measurements of RTD of water droplets in a tall-form tower having a height of 2.5 m and a diameter of 0.4. Air at a room temperature was used to minimise the complexities arising from the change in droplet size due to evaporation. The mean droplet sizes were varied from 15 μm to 125 μm. The mean droplet residence time was found to be smaller than the mean air residence time. One of the most notable studies on RTD was carried out by Kieviet (1997) using a tracer measurement technique along with CFD modelling of the drying of droplets while ignoring deposition of particles on the tower wall. The spray tower used was a short-form with a height of 3.7 m and a diameter of 2.2 m. The predicted RTD of the particles were found to smaller than the measurements. This was attributed to the assumption of neglecting deposition of particles on the wall and interaction of particles with wall/deposits. It was found that the particles spent a significant period of time in the bottom conical section and interacted with the wall in this region. Marcelo *et al.* (2003) used radiosiotrope tracer to measure the RTD of particles undergoing drying in a co-current tower. The RTD of the particles were found to be larger than the mean residence time of the air. Anandharamakrishnan *et al.* (2010) carried out CFD modelling of RTD of particles in tall- and short-form co-current spray drying towers undergoing drying. Unfortunately, no direct measurements of the particle flow behaviour and trajectories were available for comparison with the predictions.

The air and particle flow dynamics in counter-current spray drying towers are significantly different than those in co-current towers. Counter-current spray dryers involve greater levels of swirl intensity and less flow instability owing to their greater height to diameter ratios(Langrish and Fletcher, 2001; Francia *et al.* 2015a). In these towers, the smaller particles have longer residence times as they move against the air flow as opposed to co-current towers, in which the smaller particles remain in the high velocity central jet of the atomizing air and exit the tower more quickly (Kieviet, 1997; Fletcher *et al.*, 2003). Good quality experimental data of RTD are required in order to assess the adequacy of current model predictions and for the further development of the models. However, there is a dearth of such data for counter-current drying towers in the literature. The measurement of RTD of particles in a large tower is not trivial as in the actual spray drying operation the droplets with a wide size distribution undergo coalescence and agglomeration. Furthermore, particles get deposited on the wall and remain there for some time until eventually getting re-entrained back into the gas flow. A recent experimental study in a pilot-scale counter-current drying tower by Francia *et al.* (2015b) on the deposition and re-entrainment of particles on and from the wall revealed that these two phenomena drastically increase the residence times. These can lead to thermal degradation and excessive agglomeration and thus the product quality is degraded. It is not practical to validate the prediction of RTD in the tower considering all of the above mentioned processes. Therefore, evaluation of the performance of multiphase CFD in predicting RTD can be facilitated by comparing the predictions with measured RTD of dry particles in an isothermal air flow.

In this study, as a first step towards the development of a reliable CFD modelling methodology for counter-current spray dryers, the experimental measurements of the RTD of spherical glass beads in isothermal swirling air flows (without involving drying process) carried out in the pilot-scale counter-current tower, at P&G Technical Centres in Newcastle, are simulated. This tower is used for the development of detergent powder manufacturing processes. The purpose of this study is to assess how well the

Eulerian-Lagrangian approach, which is used for CFD modelling of spray drying towers in all existing studies, performs in the prediction of the RTD of the particles in strongly swirling air flows and allowing for the inclusion of the interaction of the particles with the walls of the tower. The CFD predictions are compared with the RTD data for a range of operating conditions obtained using a novel experimental technique developed for the measurement of RTD in this pilot plant tower.

2. Pilot-Scale Experimental Facilities

A schematic of the tower is given in Figure 1.

Figure – 1: Schematic of spray drying tower.

Due to the complexity of the spray drying process, the experiments were carried out in isothermal conditions, with a non-agglomerating and narrow size distribution of spherical glass beads in order to study only the effect of the swirling counter-current air flow, particle-wall interactions and injection location on the RTD of the particles. The glass beads used comprise a narrow sieve cut of sizes ranging from 300 to 425 μm and have a density of 2500 kg/m^3. This size range represents typical average detergent powder size resulting from spray drying in this tower. The size distribution of glass beads within this sieve cut was measured using a Camsizer (Retsch, 2015), which uses dynamic image analysis for the particle size measurement. The measured size distribution and the number of parcels representing each size used in the CFD simulations are listed in Table 1.

Table – 1: Size distribution of glass beads measured using Camsizer and parcels based on number fractions used in CFD simulations.

The air at an ambient temperature was injected into the spray tower using tangential-entry air inlets, which impart swirl to the flow. The pressure inside the spray tower was maintained near-atmospheric. The cone feeder depicted in Figure 2, was designed to feed the glass beads in the tower at different radial locations and heights. It has a capacity of injecting 500 g of glass beads into the tower. The time required to inject all the glass beads into the tower was measured using a high speed camera and was found to be 0.65 s, hence at a mass flow of 0.77 kg/s.

Figure – 2: Cone feeder used to inject glass beads.

Four experimental trials were carried out where the glass beads were injected at different heights and radial positions within the tower. The experimental conditions for these trials are detailed in Table 2 and the injection locations in Table 3.

Table – 2: Conditions used in trials A-D.

Table – 3: Glass beads injection locations and air mass flux in trials A-D.

To measure the RTD, the cone feeder was first filled with glass beads, and then inserted into the tower in an upright position while the air is continuously introduced into the tower. At a suitable radial location, the glass beads were dropped downwards into the up flowing air stream by simply activating a trigger to invert the feeder and at the same time manually starting a timer. The cone does not fully invert immediately, but provides time to allow the beads to freely discharge from the feeder. The timings of the mass of glass beads falling from the bottom of the tower were obtained by collecting the beads in an in-line weighing balance. It is important to note that the walls were not perfectly clean when the trials were carried out. Some patches of detergent deposits were present. Some detergent particles got entrained into the air flow during the trials;

hence the glass beads collected from the tower bottom also contained detergent particles, which added to the mass of the glass beads collected and hence resulted in measurement error, which could not be avoided. Another limitation of this method is that it was not possible to measure the residence time of individual particle sizes.

3. CFD Modelling Methodology

For the simulation of the RTD experiments, an isothermal Eulerian-Lagrangian multiphase CFD modelling approach is used. The Reynolds-averaged continuity and Navier-Stokes equations together with turbulence model equations are solved for the gas phase using the CFD software Fluent v. 14.5 (details can be found in Ali *et al*., 2016 and Fluent, 2014). The turbulence is modelled using the Reynolds-stress transport model which utilizes the linear pressure-strain model of Launder *et al.* (1975). The selection of this turbulence model was based on a comprehensive validation of the predicted mean and fluctuating air velocity profiles in this tower against experimental data carried out by Ali (2014). Measurements were carried out as part of an experimental program and data were reported in Francia et al. (2015a). Generally, a good level of agreement between the predictions and measurements was obtained using steady state conditions. Furthermore, a comparison was made between the air velocity profiles obtained using steady and transient flow calculations and the predicted profiles were found to be similar. The computational mesh used in the calculations was selected through extensive mesh independent tests against measured air velocity data and it comprises 1.3×10^6 tetrahedral cells (Ali, 2014). The measured mass flow rate of air (see Table 2) was specified at the inlet faces of the tangential-entry air inlets as the inlet boundary condition. The pressure outlet boundary condition was specified at the top outlet of the tower with a value of -300 Pa. For the modelling of near-wall flow, a no-slip boundary condition together with the log-law of the wall was used. The uncleaned tower wall was approximated as a rough wall with a uniform roughness height of 2 mm throughout the tower (Ali, 2014). The governing equations for fluid flow were discretised using the finite-volume method. The second-order upwind discretisation scheme (described in Versteeg and Malalasekera, 2007) was used for the convective

terms. For the pressure-velocity coupling the PISO scheme (Issa, 1985) and for the pressure interpolation, PRESTO! scheme (see Versteeg and Malalasekera, 2007) were used.

Once the air flow simulation suitably converged, the particles were introduced in the calculation. The trajectories of representative particles are calculated by solving the equation of motion using the Lagrangian approach. The dispersion of particles due to gas phase turbulence is taken into account using the discrete random walk model of Hutchinson *et al.*, (1971). For the calculation of drag force, the drag law of Morsi and Alexander (1972) which is applicable to smooth spherical particles is used. For the particle-wall interaction, both smooth wall and rough wall scenarios are considered. In the smooth wall scenario, a constant restitution coefficient of 0.7 is used. In the case of rough wall, the effect of wall roughness on particles post-wall collision trajectories is modelled using the rough-wall collision model described in Ali *et al.* (2015). In this approach, the rough wall is represented by a series of rough surfaces and the roughness inclination angles to which the particles collide are generated stochastically assuming a Gaussian distribution. This model was implemented in the calculation using user-defined functions feature in Fluent. Particle-particle interactions are ignored in all the simulations.

In the calculation, particles were injected in a hollow cone pattern to replicate the discharge of glass beads from the cone feeder (see Figure 2). The initial axial and radial velocity components of all the particles are set to 0 m/s as the particles are initially at rest; when the cone is inverted, they fall due to gravity. The total number of parcels representing the particles of different sizes when all the glass beads are injected is 650,000 (see Table 1). The height of injection, the mass flow and the duration of injection of glass beads are given in Table 2 and 3. Since a batch of fixed mass of particles are injected during a fixed length of time; therefore, it is necessary to track all the particles in the batch simultaneously in time. This requires a transient simulation of air flow with a two-way momentum coupling, which is computationally expensive. Therefore, to optimize the computation time, a sensitivity study was carried out to assess the influence of time step (Δt) used for the

transient calculation of the continuous phase as well as for the tracking of particles on the predicted results. The effect of Δt on the residence time of particles is depicted in Figure 3. The simulation with Δt = 0.1 s and 0.01 s took about 3.5 hours and 24 hours of computation time, respectively, for all the particles to exit from the tower. For the simulation with Δt = 0.001 s, the computation was carried out for about 10 s of real time which took 4 days, but not all the particles exited the tower during this period. The simulation with Δt = 0.0005 s was continued until all particles exited the tower, which took about 10 days of computation time. The predicted RTD plot with Δt = 0.01 s has an offset of about 1 s compared to that with Δt = 0.001 s, whereas the predicted RTDs obtained with Δt = 0.001 s and 0.0005 s match very well. Hence Δt = 0.001 s is an optimum time step size which was used in all transient simulations.

Figure – 3: Sensitivity of Δt on the predicted RTD curve.

The use of a large number of parcels (each about 10% of the total number of glass beads injected) ensured that the results are statistically representative. The computation time required for particle tracking was relatively smaller compared to the continuous phase calculation; therefore, no sensitivity study was carried out to optimise the number of parcels representing the discrete phase as this would not result in an appreciable reduction in the overall computation time. The time at which each parcel exits from the bottom of the tower, along with its mass, was recorded using a user-defined function feature. Hence a plot of cumulative mass collected as a function of time was obtained using this data which was then compared with measurements.

Three modelling approaches (referred to as cases 1-3) were used to simulate trial A in order to assess the effect of wall surface conditions and the inlet particle size on the predicted RTD. These are listed in Table 4.

Table – 4: Modelling cases for trial A.

Computations were carried out on a 2.4 GHz octa-core processor and the computation time for cases 1 and 2 was about 24 hours each, whereas for cases 2 and 3 was around 5 days each.

4. Results and Discussion

RTD of Trial A

The predicted RTD in the form of cumulative mass of glass beads collected from the tower bottom for various simulated cases (see Table 4) are compared with the measurement for trial A in Figure 4. S-shaped curves can be observed in all the simulated cases as well as in the measurement. The point at which the curve starts to rise represents the time at which particles start to exit the tower bottom and the y-axis represents the amount of mass collected at the tower bottom with time. Once all the particles have exited the tower, the curve becomes flat. In the experimental data, the cumulative mass collected after 15 s is about 480 g. The remaining 20 g of glass beads might still be in the tower or might have been entrained by the air and left from the top exit of the tower. However, the CFD predictions do not show entrainment of particles by the air flow. No measurement of particle collected at the top exit is available to corroborate this. Case 1 (considering smooth wall for particle-wall interaction) results in a relatively narrow RTD (steeper RTD curve) compared to case 2 in which the rough wall collision model is used. The roughness at the wall results in a wider spread of RTD and gives closer qualitative representation of the measured RTD trend. In case 3, the RTD prediction with the rough wall collision model, in which the measured particle size distribution is used instead of an average size as in case 2, provides the closest agreement with the measurement, with a maximum deviation of 1 s. It should be noted that the measurement includes human error incurred in manually starting the timer when the glass beads were injected into the tower. Disagreement between the predictions of case 2 (average size) and case 3 (measured size distribution) reveals that even though a narrow sieve fraction of glass beads was used, the average size is not representative of the actual size distribution ranging from 300 to 425 μm.

Figure – 4: Measured and predicted mass of beads collected from the bottom exit v/s time for trial A.

Particle Trajectories

In Figure 5, the location of beads of various sizes (coloured by diameter) in the tower predicted using case 3 is depicted. It is observed that the largest sizes exit first followed by the smaller ones. This is expected as larger particles have a greater gravitational to drag force ratio, and are less influenced by turbulence compared to the smaller sizes.

Figure – 5: Predicted location of beads of different sizes (coloured by diameter) for trial A and case 3.

Figure 6 is a plot of predicted concentration of beads along the diameter of the tower after 6 s of simulation time at a dimensionless height $z/Z = 0.2$ for case 3. It can be observed that the concentration is very high near the wall and almost negligible in the central region of the tower. This is due to the beads swirling downwards through the swirling flow of air upwards and the centrifugal force forces them to concentrate near the wall.

Figure – 6: Predicted bead concentration distribution along the radius at $z/Z = 0.2$.

RTDs of Trials B-D

Further validation of the predicted RTD is carried out by simulating the experimental trials B, C and D conducted by injecting glass beads at different heights and radial positions within the tower. These operating conditions are listed in Tables 2 and 3. The modelling methodology of case 3 in trial A is used for simulating these trials.

In trial B, the radial location (r) of glass beads injection was changed to $r/R = 0.5$, while the height and air flow was kept the same as in the base case trial A. In trial C, the height of injection was lowered to $z/Z = 0.4$, but the radial location and the air mass flow were unchanged. In trial D, the injection height and radial location was the same as in trial A, whereas the air mass flux was increased to 1.47 kg/m^{2}s to assess the

influence of increased air velocity on the RTD, which is expected to increase the local concentration of glass beads.

Figure 7 is a plot of the predicted and measured residence times of the glass beads for trial B conditions. There is a maximum offset of about 2 s between the predictions and measurements. Measured values of the RTD for trial A are given also for comparison with the trial B measurements. The beads start to come out about 1 s earlier in trial B compared to trial A. Since the height and air mass flow are the same in both trials, changing the injection radial location to off-centre causes an asymmetric flow of the glass beads. This may have increased the localized concentration of glass beads hence causing more clustering and resulting in a smaller drag force on individual particles. The CFD predicted RTD do not change significantly by changing the radial location of the injection. This could be attributed mainly due to the clustering effect of glass beads on the drag coefficient, but this is ignored in the CFD simulation.

Figure – 7: Measured and predicted mass of beads collected from the bottom v/s time for trial B.

Figure 8 is a plot of the measured and CFD predicted RTD of the glass beads for trial C together with the measured RTD plot of trial A for comparison. In this case, since the particles are injected at a lower height compared to trial A, while the air flow is the same, it is expected that the particles would start to leave the tower earlier, which happens in both the measurements and predictions. However, the measured initial time at which beads start to exit the tower is not significantly different in trials A and C, and only an offset of 1 second is observed. The CFD model predicts the initial exit time to be 3 seconds compared to the measurement of about 5 s. In the trends obtained in trials A and B, the predicted initial times were greater than the measured values. However, in this trial the predicted start time of beads exiting the tower is shorter than the measurement. This discrepancy could be mainly due to ignoring particle-particle interaction in the CFD simulation, which may be particularly important in the bottom conical region of the tower. The beads

roll down the conical wall and interact with each other more strongly in this case since the distance between the injection location and the conical region is smaller. Hence the beads are less dispersed along the height when they reach the conical region, therefore a larger concentration of beads occurs on the conical wall will lead to more particle-particle collisions and increased resistance to particles movement.

Figure – 8: Measured and predicted mass of beads collected from the bottom v/s time for trial C.

In trial D, the mass flux of air is increased from 0.98 kg/m^{2}s to 1.47 kg/m^{2}s. The measured and predicted residence times for this case are depicted in Figure 9. As can be seen, the predicted RTD is significantly different from that measured. In the measured data, the beads start to come out of the tower at about 6 seconds and after about 20 s, all have exited the tower. The cumulative residence time distribution predicted by CFD indicates that the beads start to exit the tower after about 10 s and two S-shaped curves are observed. The largest beads (~500 μm) exit first and after some time (~20 s) the smaller ones start to exit the tower. The total mass of glass beads that exited the tower in the CFD simulation was about 250 g at the end of 65 s of simulation time, the remaining 250 g particles were still in the tower. The simulation run was stopped at that time. The large difference in the predicted and measured residence time for this case requires further probing including the effect of clustering on the effective drag force on beads.

Figure – 9: Measured and predicted mass of beads collected from the bottom v/s time for trial D.

5. Conclusions

A multiphase CFD modelling study has been carried out to predict the RTD of particles in a pilot-scale counter-current spray drying tower and the predictions were compared with the measured RTD data. It is found that the modelling of particle-wall collision plays an important role in predicting the dispersion of particles in the tower. Consideration of wall roughness for particle-wall collision provides a better qualitative

agreement with the measurement. A good agreement is obtained between the predicted and measured RTD for trials A and B where beads were injected at two different radial locations. In trial C with a lower injection height, CFD predicts shorter residence times compared to the measurements with a maximum deviation of 3 s. However, a significant discrepancy between the predicted and measured RTD is observed for trial D with a higher air flow and this requires further investigation. The analysis of the experimental data infers that the clustering effect of the particles on reducing the drag force may be important. Hence the effect of clustering of particles on the effective drag coefficient should be evaluated. Consideration should also be given to particle-particle collision especially in the bottom conical region of the tower thus necessitating the used of four-way coupling, particularly when the particle loading in the tower is high. Overall, a good quantitative reproduction of the measured RTDs using CFD predictions is obtained for the trials with a low air mass flow but a significant discrepancy was found at a higher air flow.

Acknowledgement

Financial support provided by Innovate UK (formerly Technology Strategy Board) (20891-138269) through the Engineering and Physical Sciences Research Council, (TS/K00252X/1) is gratefully acknowledged.

References

Ali, M. (2014). CFD modelling of a counter-current spray drying tower. PhD Thesis, University of Leeds, UK.

Ali, M., Mahmud, T., Heggs, P., Ghadiri, M., Bayly, A., Hossein, A. and MartindeJuan, L. (2015). CFD Simulation of a counter-current spray drying tower with stochastic treatment of particle-wall collision. Procedia Engineering, vol. 102, pp. 1284 – 1294.

Anandharamakrishnan, C., Gimbun, J., Stapley, A. G. F. and Rielly, C. D. (2010). A Study of Particle Histories during Spray Drying Using Computational Fluid Dynamic Simulations. Drying Technology, vol. 28(5), pp. 566 - 576.

Crowe, C. T. (1983). Droplet-gas interaction in counter-current spray dryers. Drying Technology, vol. 1, pp. 35-56.

Fletcher, D., Guo, B., Harvie, D., Langrish, T., Nidjam, T. andWilliams, J. (2003).What is important in the simulation of spray dryer performance and how do current CFD models perform? Third international conference on CFD in Minerals and Process Industries CSIRO, Melbourne, Australia, pp. 357-363.

Fluent, Ansys Inc. User Guide 2014.

Francia, V., Martin, L., Bayly, A. E. and Simmons, M. J. H. (2015a). An experimental investigation of the swirling flow in a tall-form counter current spray dryer. Exp. Therm. Fluid Sci., vol. 65, pp. 52-64.

Francia, V., Martin, L., Bayly, A. E. and Simmons, M. J. H. (2015b). The role of wall deposition and re-entrainment in swirl spray dryers. J. AIChE, vol. 61 (6), pp. 1804-1821.

Hutchinson, P., Hewitt, G. F. and Dukler, A. E. (1971). Deposition of liquid or solid dispersions from turbulent gas streams: a stochastic model. Chem. Eng. Sci., vol. 26, pp. 419-439.

Issa, R. I. (1985). Solution of the implicitly discretised fluid flow equations by operator splitting. J. Comp. Phy., vol. 62, pp. 40-65.

Jaskulski, M., Wawrzyniak, P. and Zbicinski, I. (2014). CFD model of particle agglomeration in spray drying. 19th International Drying Symposium (IDS 2014), France.

Kieviet, F. G. (1997). Modelling quality in spray drying. PhD Thesis, Edinhoven University of Technology, The Netherlands.

Langrish, T. A. G. and Fletcher, D. F. (2001). Spray drying of food ingredients and applications of CFD in spray drying. Chem. Eng. Proc., vol. 40, pp. 345-354.

Launder, B. E., Reece, G. J. and Rodi, W. (1975). Progress in the development of a Reynolds-stress turbulence closure. J. Fluid Mech., vol. 68, part 3, pp. 537-566.

Livesley, D. M., Oakley, D. E., Gillespie, R. F., Ranpuria, C. K., Taylor, T., Wood, W. and Yeoman, M. L. (1992). Development and validation of a computational model for spray-gas mixing in spray dryers. Drying ’92, Ed. Mujumdar, A. S., pp. 407-416, New York: Hemisphere Publishing Corp.

Masters, K. (1985). Spray Drying Handbook. London: Leonard Hill Books.

Mazza, M. G. G., Brandão, L. E. B. and Wildhagen, G. S. (2003). Characterization of the Residence Time Distribution in Spray Dryers, Drying Technology, vol. 21 (3), pp. 525-538.

Morsi, S. A. and Alexander, A. J. (1973). An investigation of particle trajectories in two phase flow systems. J. Fluid Mech., vol. 55, pp. 193-208.

Pham, Q. T. and Keey, R. B. (1977). Some experiments on the residence time distribution of droplets in a cocurrently worked spray chamber. The Canadian Journal of Chemical Engineering, vol. 55, pp. 466-470.

Retsch. (2015). http://www.retsch-technology.com, Accessed: 22-09-2015.

Versteeg, H. K. and Malalasekera, W. (2007). An Introduction to Computational Fluid Dynamics; Pearson Education Ltd.: Harlow, England, second edition, 2007.

Wawrzyniak, P., Podyma, M., Zbicinski, I., Bartczak, Z., Polanczyk, A. and Rabaeva, J. (2012). Model of heat and mass transfer in an industrial counter-current spray-drying tower. Drying Technology, vol. 30, pp. 1274-1282.

Wawrzyniak, P., Jaskulski, M., Zbicinski, I. amd Podyma, M. (2014). Two phase CFD model of a counter-current spray drying process. 19th International Drying Symposium (IDS 2014), France.

Zbicinski, I. and Zietara, R. (2004). CFD model of counter-current spray drying process. Drying 2004, São Paulo, Brazil, vol. A, pp. 169-176.

Table – 1: Size distribution of glass beads measured using Camsizer and parcels based on number fractions used in CFD simulations.

Diameter (µm)	Mass Fraction	Mass (kg)	Numbers	Number Fraction	Parcels
321	0.042	0.021	485273	0.072	46772
370	0.534	0.267	4028911	0.597	388322
412	0.384	0.192	2097321	0.311	202148
491	0.041	0.021	132370	0.020	12758
Total	1	0.5	6743875	1	650000

Table – 2: Conditions used in trials A-D.

Parameter	Value
Outside diameter of the feeder (D_o)	0.187 m
Total mass of glass beads injected	0.5 kg
Duration of injection of glass beads	0.65 s
Mass flow of glass beads	0.77 kg/s
Envelope density of glass beads	2500 kg/m^3
Bulk density of glass beads	1500 kg/m^3
Air mass flux	0.98 & 1.47 kg/m^{2}s

Table – 3: Glass beads injection locations and air mass flux in trials A-D.

Experiment	Injection Height (z/Z)	Radial Position (r/R)	Air Mass Flux (kg/m^{2}s)
Trial A (base case)	0.58	0 (centre)	0.98
Trial B	0.58	0.5 (off-centre)	0.98
Trial C	0.4	0 (centre)	0.98
Trial D	0.58	0 (centre)	1.47

Where z = injection height, Z = total tower height, r = radial position and R = tower radius

Table – 4: Modelling cases for trial A.

Case	Glass beads size	Particle-wall interaction model	Momentum coupling
1	D_{avg} = 362 µm	Smooth wall, C_r = 0.7	Two-way
2	D_{avg} = 362 µm	Rough wall collision model (Ali *et al.*, 2015)	Two-way
3	Measured size distribution (see Table 1)	Rough wall collision model	Two-way

Where D_{avg} = arithmetic average size¸ C_r = restitution coefficient

Figure – 1:

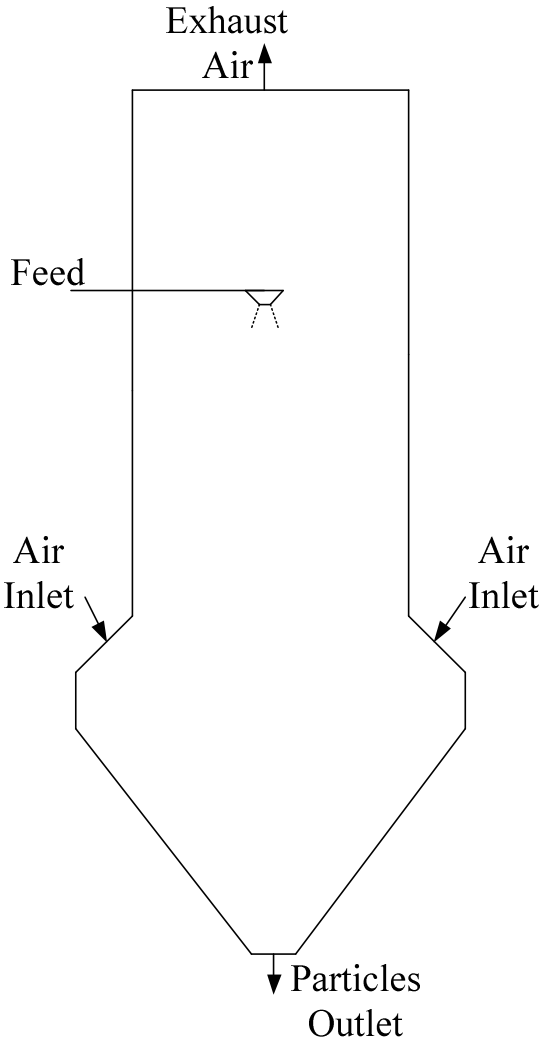

Figure – 1: Schematic of spray drying tower.

Figure – 2:

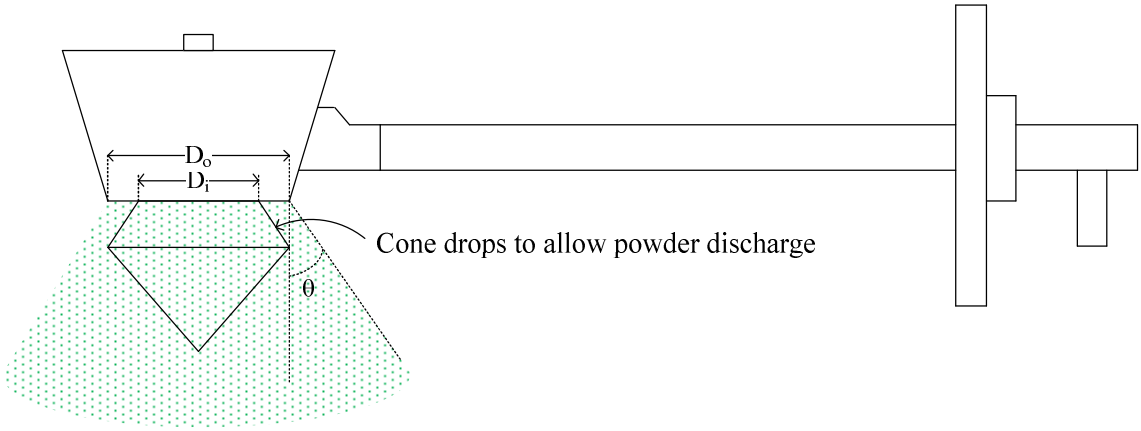

Figure – 2: Cone feeder used to inject glass beads.

Figure – 3:

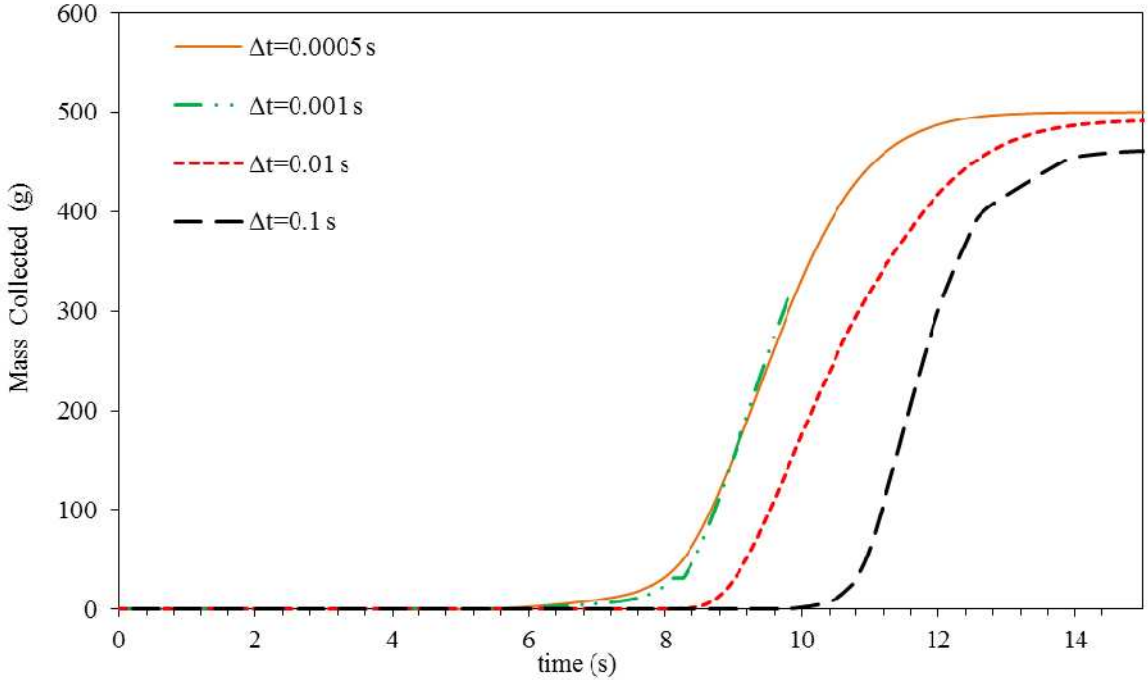

Figure – 3: Sensitivity of Δt on the predicted RTD curve.

Figure – 4:

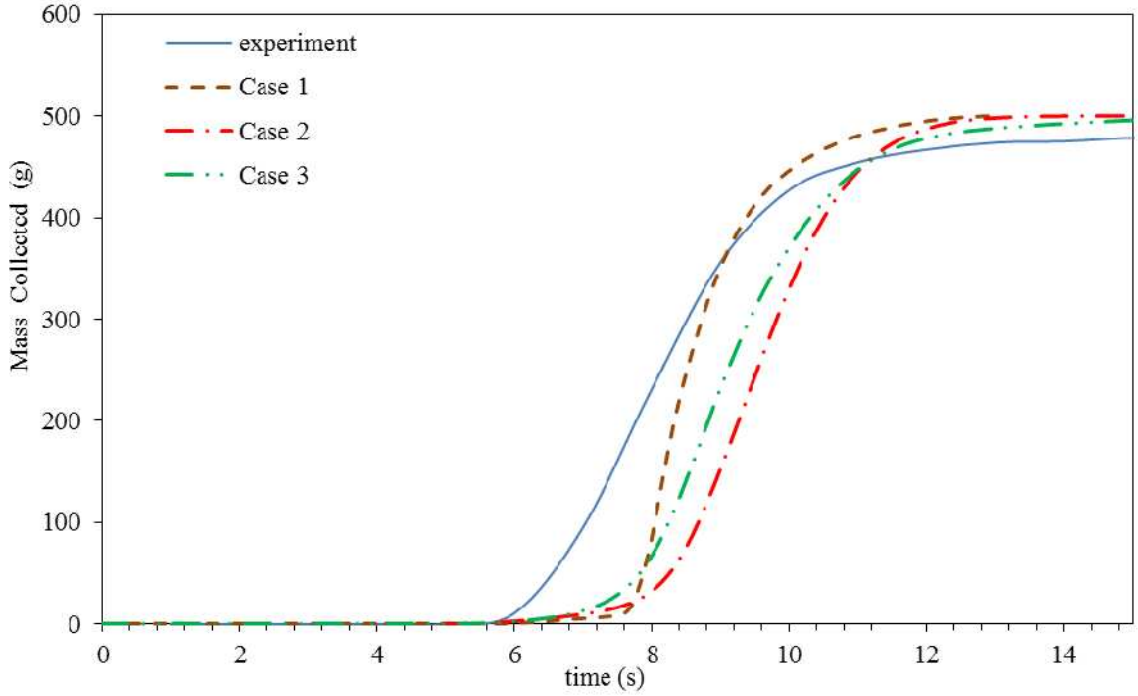

Figure – 4: Measured and predicted mass of beads collected from the bottom exit v/s time for trial A.

Figure – 5:

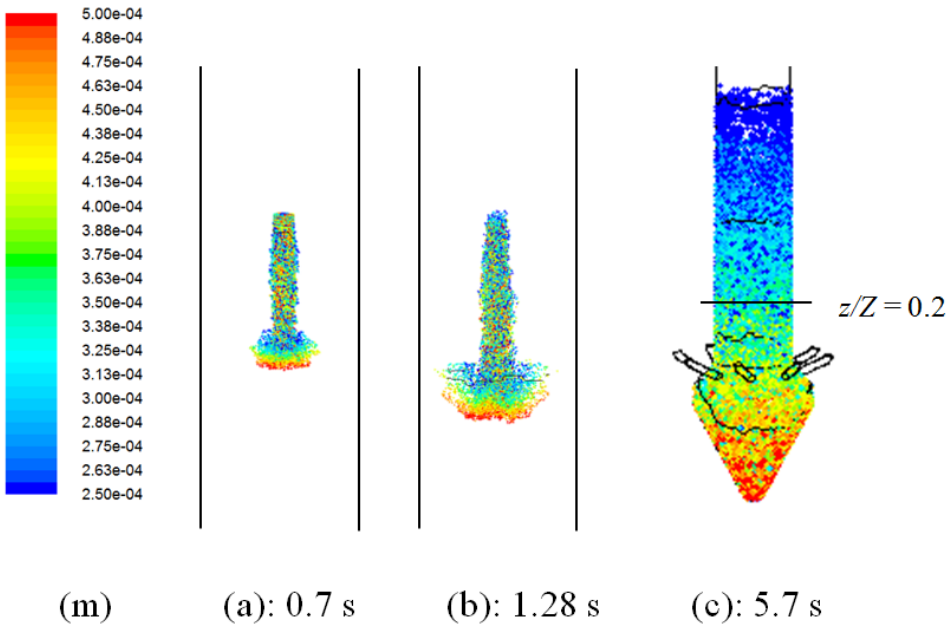

Figure – 5: Predicted location of beads of different sizes (coloured by diameter) for trial A and case 3.

Figure – 6:

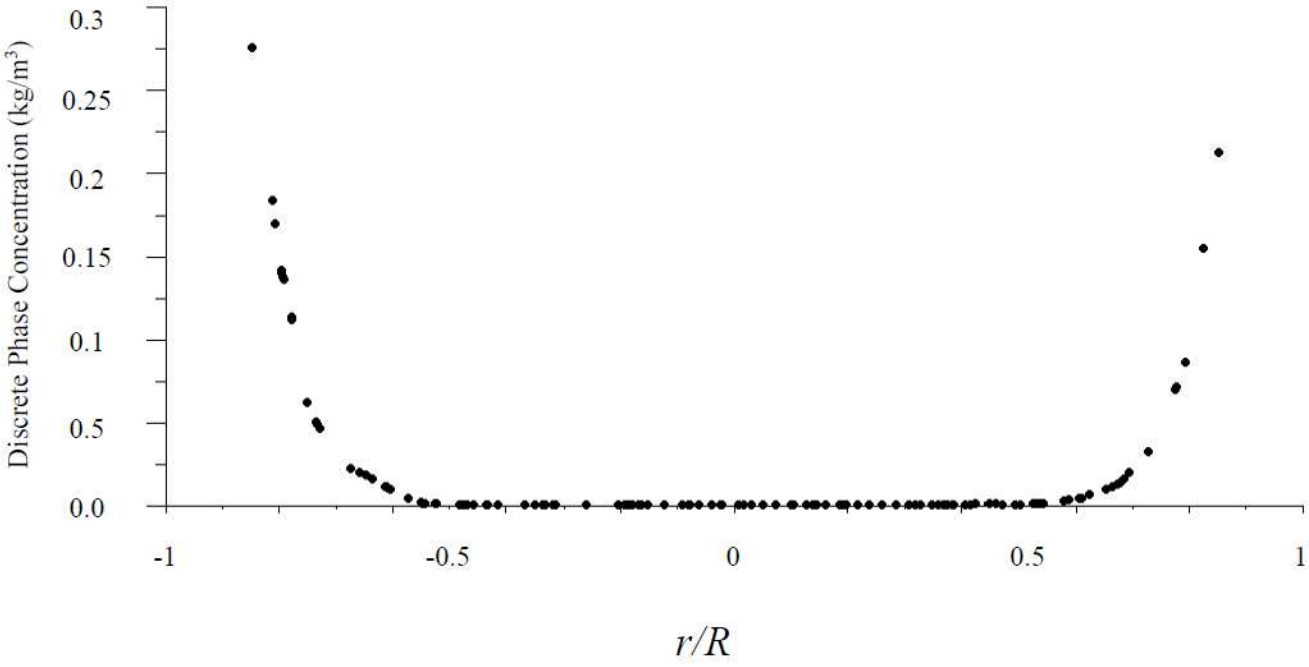

Figure – 6: Predicted bead concentration distribution along the radius at $z/Z = 0.2$.

Figure – 7:

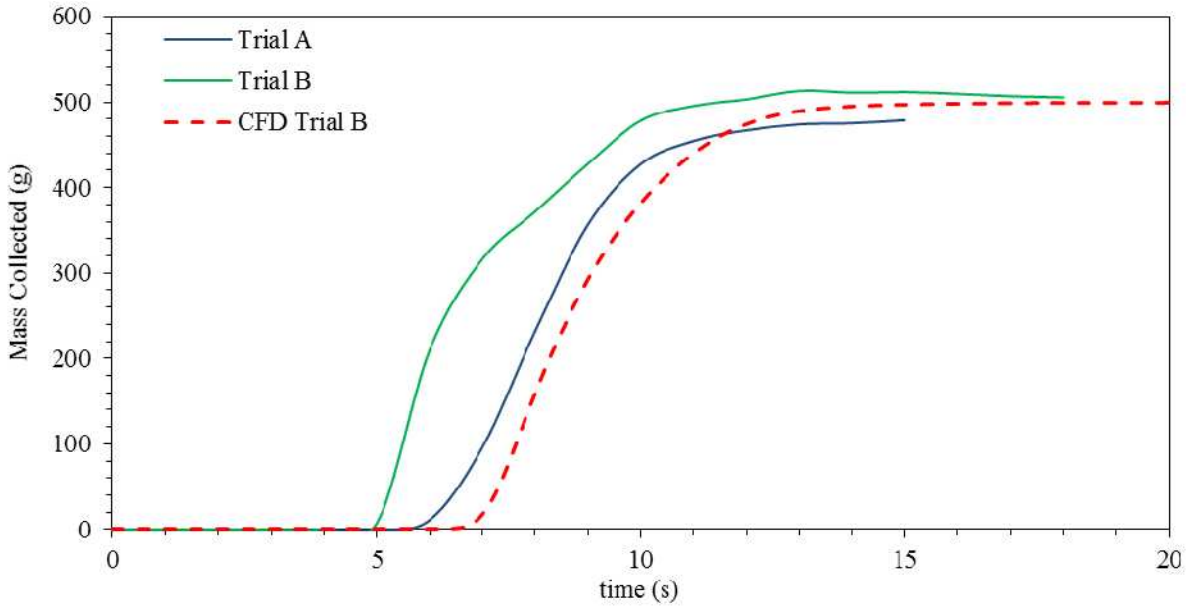

Figure – 7: Measured and predicted mass of beads collected from the bottom v/s time for trial B.

Figure – 8:

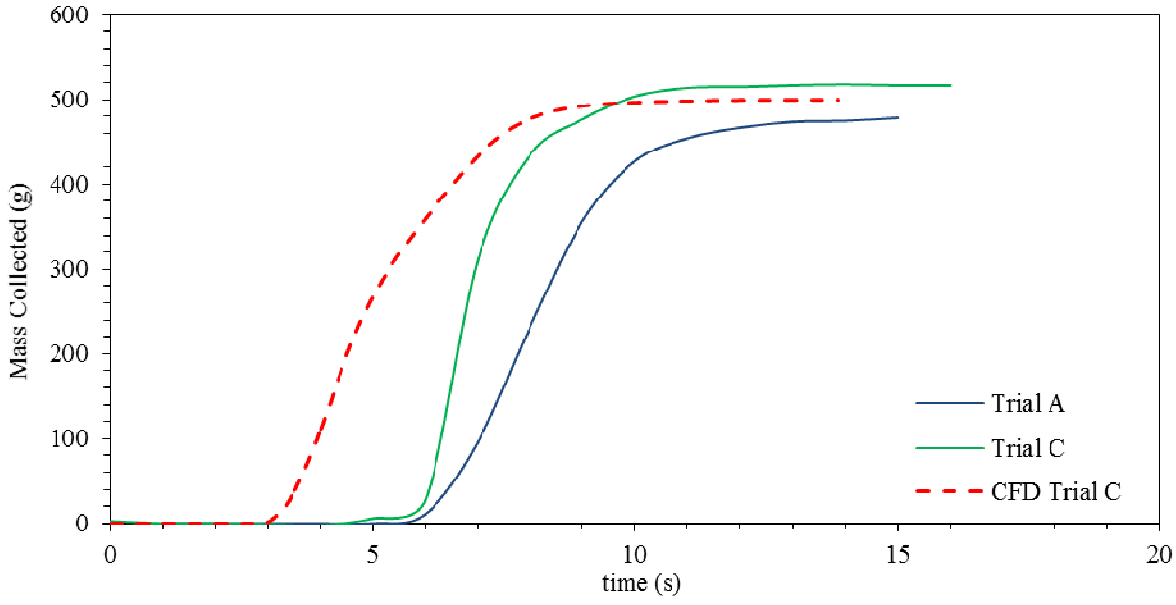

Figure – 8: Measured and predicted mass of beads collected from the bottom v/s time for trial C.

Figure – 9:

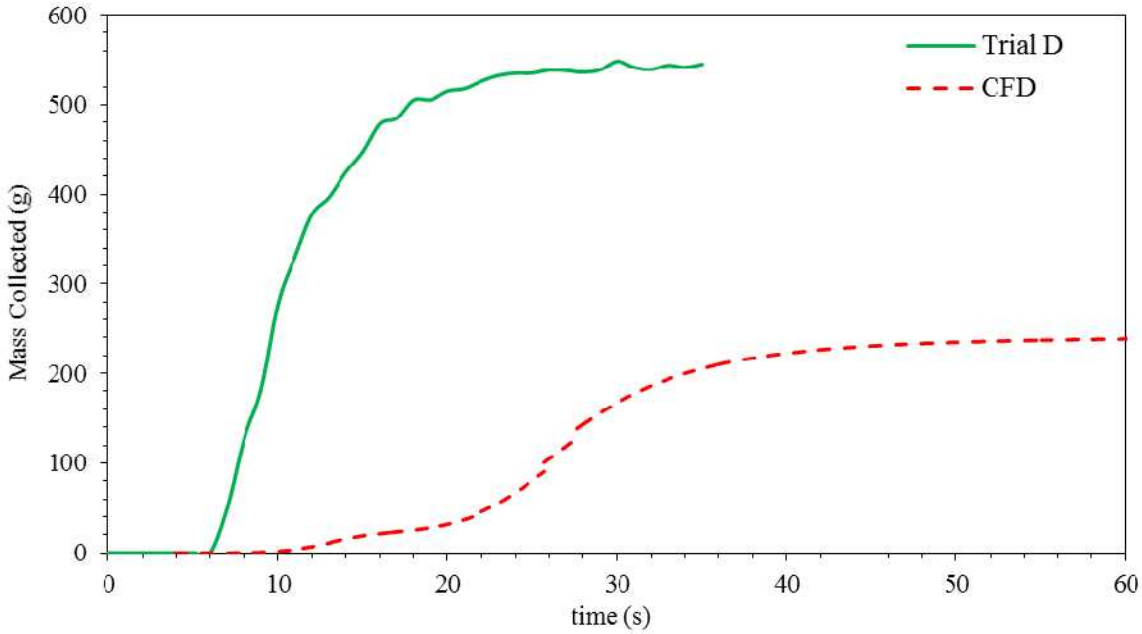

Figure – 9: Measured and predicted mass of beads collected from the bottom v/s time for trial D.